Microsatellite instability in aberrant crypt foci from patients without concurrent colon cancer

Emily J.Greenspan[1], Jennifer L.Cyr[2], Devon C.Pleau[2],
Joel Levine[2,3], Thiruchandurai V.Rajan[2,4],
Daniel W.Rosenberg[1,2] and
Christopher D.Heinen[2,*]

[1]Center for Molecular Medicine, [2]Colon Cancer Prevention Program,
Neag Comprehensive Cancer Center, [3]Division of Gastroenterology and
[4]Department of Immunology and Pathology, University of Connecticut
Health Center, Farmington, CT USA

*To whom correspondence should be addressed.
Email: cheinen@uchc.edu

Aberrant crypt foci (ACF) are microscopic surface abnormalities that are putative precursors to colorectal cancer (CRC). ACF exhibit similar histological and molecular abnormalities to adenomas and CRC and potentially represent useful biomarkers of cancer risk. Microsatellite instability (MSI) is one molecular abnormality identified in concurrent ACF from CRC patients that may indicate a risk for progression. To determine if MSI can be detected in ACF from cancer-free subjects, we examined 45 ACF from 20 subjects undergoing colonoscopies. The group included 12 patients at elevated risk for CRC based on family history of CRC or personal history of CRC or advanced adenoma and 8 patients with no known risk factors. ACF were identified using close-focus magnifying chromendoscopy and collected by biopsy *in situ*. Genomic DNA was prepared from ACF and adjacent normal colonic epithelium isolated by laser capture microdissection and analyzed for MSI. MSI was identified in at least one marker from 9 of 30 (30%) lesions from patients at elevated risk for CRC and in 2 of 15 (13%) lesions from average risk patients. Using methylation-specific PCR analysis, we also examined the ACF for promoter hypermethylation of the DNA repair genes *hMLH1* and *MGMT* and found moderate changes (8/39 and 3/32, respectively). Although we found only a limited relationship between *hMLH1* hypermethylation and MSI, all the lesions with *MGMT* hypermethylation displayed an MSI-low phenotype. These lesions may be precursors to MSI-low CRC, providing a potential early biomarker to assess the effects of cancer prevention strategies.

Introduction

Screening for early detection of colorectal adenomas is currently considered the most effective means of preventing colorectal cancer (CRC)-related death. Aberrant crypt foci (ACF) are postulated to be a precursor to the adenoma in the step-wise progression of CRC, and thus, potentially represent

Abbreviations: ACF, aberrant crypt foci; CRC, colorectal cancer; LOH, loss of heterozygosity; MSI, microsatellite instability; MSP, methylation-specific PCR.

an earlier biomarker for cancer risk. ACF are microscopic surface abnormalities first identified in carcinogen-treated rodents and later in human colon (1,2). In animal models, ACF have been used as biomarkers to study the potency of colon carcinogens, as well as the effectiveness of chemopreventive agents (3). In human colon, they may also serve as a useful biomarker for determining cancer risk or response to cancer prevention strategies. With the advent of close focus high-magnification chromoendoscopy, ACF can now be detected *in situ* and biopsied during a colonoscopy examination. This advance allows for a more complete characterization of these lesions to determine their suitability as a biomarker for CRC.

ACF display histologic features and molecular abnormalities in common with colonic adenomas and CRC supporting the notion that these lesions are the first step in the colon cancer progression pathway (3–8). An important question in the study of ACF is whether one can identify gross, histological or molecular features indicative of an increased risk for progression. Microsatellite instability (MSI) is one molecular abnormality identified in ACF that may indicate such a risk. MSI is a form of genomic instability at simple repeat sequences in the genome and is a hallmark of defective DNA mismatch repair (MMR) (9). MSI has been detected in 10–30% of sporadic CRC (10), as well as in greater than 95% of tumors from hereditary non-polyposis colon cancer (HNPCC) patients (11). Previous studies have identified MSI+ ACF (ACF that display instability of one or more microsatellite markers) from resected colon tissue obtained during surgery for a concurrent colon cancer (12–15). This observation suggests that loss of MMR function may occur very early in the tumorigenic process. However, as the ACF to carcinoma progression likely takes several years (16), MSI+ ACF should be detectable in patients in advance of cancer development.

The following study was undertaken to determine whether MSI+ ACF could be identified within the colons of individuals without a concurrent cancer by examining lesions biopsied *in situ* from patients undergoing screening or surveillance colonoscopy. Our data indicate that MSI can be detected in ACF from patients without a concurrent cancer. Interestingly, there is a slight increase in the percentage of MSI+ ACF in patients who had either (i) a previous advanced adenoma/colon cancer, or (ii) a first-degree relative with CRC compared to those with no known personal or family history of CRC. We also detected promoter hypermethylation of the DNA repair genes *hMLH1* and *MGMT* in ACF. While we did not see a clear correlation between MSI and *hMLH1* promoter methylation status, we did identify MSI in all ACF with *MGMT* promoter hypermethylation. By identifying these molecular aberrations in ACF from patients without a concurrent cancer, follow-up studies may be possible to determine the predictive value of these lesions for cancer risk.
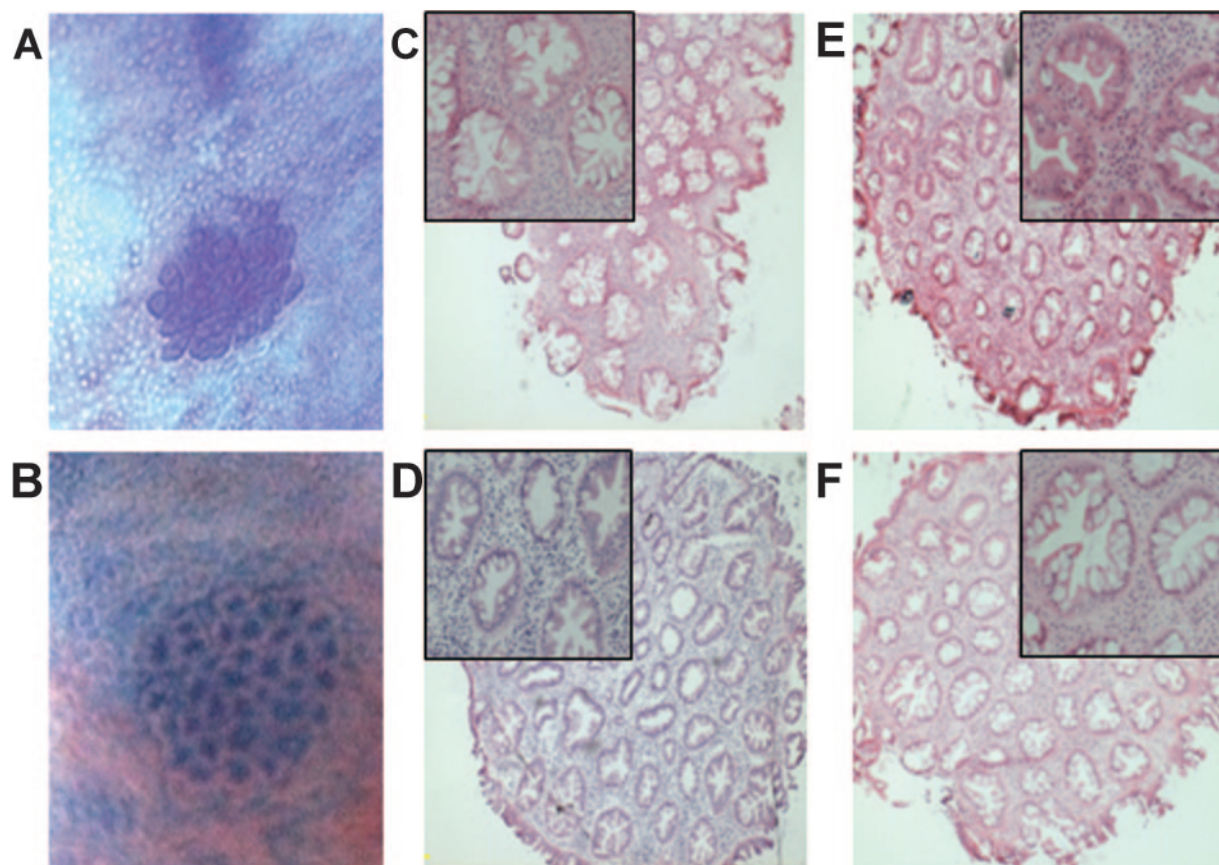
Fig. 1. Macroscopic and histologic comparisons of ACF. (**A** and **B**) Gross views of ACF visualized through the Olympus close-focus colonoscope at ×60 magnification. The mucosa was stained with 0.5% methylene blue. (**C–F**) Cross-sectional views of H&E stained frozen sections of hyperplasic ACF at ×40 and ×200 (inset detail) magnification. The serrated lumen pattern, characteristic of hyperplastic lesions, is readily apparent.

Materials and methods

Subject selection

Two groups of patients were included in this study; those considered at elevated risk for CRC and those considered at average risk for CRC. Elevated risk was based on a positive family history (at least one first degree relative with the disease) and/or a positive personal history for CRC or advanced adenomas (17,18). Subjects designated as average risk for CRC indicated no personal or family history of CRC or benign polyps/adenomas. Patients suspected of having familial adenomatous polyposis or HNPCC (based on Amsterdam criteria) were excluded from this study. Patients underwent total colonoscopy at the John Dempsey Hospital (JDH) at the University of Connecticut Health Center (UCHC) in accordance with insti- tutional policies. This study was performed after approval by an Institutional Review Board and all subjects provided written informed consent.

ACF collection and characterization

ACF were isolated from grossly normal appearing colonic mucosa by biopsy *in situ* during the high-resolution close-focus chromendoscopy portion of the total colonoscopy procedure performed in the JDH at UCHC. The distal 20 cm of colon including the rectum was examined after washing with 10– 20 ml of 20% *N*-acetylcysteine followed by water wash to remove surface mucus. Then, a freshly prepared solution of 0.5% methylene blue was applied for contrast staining using spray catheters. After a waiting period of at least 2 min for vital dye–epithelial cell interaction, high volume water wash was applied. The maximum volume of the dye applied to the mucosa was 40 ml. Dye was only applied to the colorectal mucosa being studied. ACF were visualized and photographed using an Olympus Close Focus Colonoscope (XCF-Q160ALE), which enables visualization from 2 to 100 mm at a magnifying power of ×60 (Figure 1A and D) (7). Under close focus magnification, a finding was accepted as an ACF if 2 or more crypts had increased lumen diameter of 1.5 to ×2 compared to surrounding crypt lumens, if lumen shape was round, dilated or slit (non-hyperplastic), serrated (hyperplastic), or with thick crypt walls with compressed lumens (dysplas- tic). On tangential view, ACF were required to be raised above the mucosal

surface. The endoscopist (J.L.) and two technicians trained in ACF image morphology observed the endoscopic image. The observers had to be in agreement that the lesion met the previously described criteria of ACF to be entered into study. Per protocol, a maximum of 12 biopsy specimens of ACF were taken within the distal 20 cm using forceps (Precisor EXL, CR Bard). Biopsies of individual ACF were embedded immediately in tissue freezing medium (OCT) and stored at −80°C. Frozen serial sections of ACF were prepared at 5–7 μm thickness on glass slides. Representative frozen sections of ACF were stained with hematoxylin and eosin for routine histological analysis by light microscopy of coded specimens by a pathologist (T.V.R.) (19,20).

DNA extraction

Frozen sections of ACF were stained and dehydrated using the Histogene staining kit (Molecular Devices, Sunnyvale, CA, USA), according to the manufacturer's instructions. Laser capture microdissection (LCM) was performed on prepared sections using the Veritas LCM system (Molecular Devices). Whenever possible, adjacent normal mucosal cells directly abutting the aberrant crypts were collected separately by laser capture. On average, 1500–3000 cells were collected from each sample. DNA was extracted using the Picopure DNA extraction kit (Molecular Devices) and quantified using Picogreen (Molecular Probes, Eugene, OR, USA).

Cell lines and culture conditions

DNA was isolated from three established colon cancer cell lines, SW480, SW48 and RKO. RKO cells were grown in minimum essential medium (Eagle) (Invitrogen, Carlsbad, CA), supplemented with 10% fetal bovine serum (FBS) and 5% penicillin/streptomycin. SW480 and SW48 cells were grown in Dulbecco's modified Eagle's medium (Invitrogen), supplemented with 10% FBS and 5% penicillin/streptomycin.

MSI and loss of heterozygosity analysis

For MSI analysis, DNA was isolated from microdissected ACF and matched adjacent normal colon epithelia. MSI status was determined in all samples using the National Cancer Institute (NCI) recommended panel of five

microsatellite markers (BAT25, BAT26, D2S123, D5S346 and D17S250) (21) plus three additional microsatellite sequences found within the coding regions of *TGFβRII*, *hMSH3* and *hMSH6* (22). An ACF was considered to be MSI-high if three or more markers were positive for novel alleles compared to matched normal DNA, MSI-low if two or less markers were positive and microsatellite stable if none of the markers were positive.

PCR for all microsatellites were carried out using the forward oligonucleotide dye-labeled method using WellRED oligos (Proligo, Boulder, CO, USA). DNA was amplified in 10 μl volumes containing ×1 PCR buffer (Roche), 1 nmol each deoxynucleotide (Invitrogen), 0.25 U *Taq* polymerase (Invitrogen), 5 pmol of the forward fluorescently labeled primer (Proligo), 5 pmol of the reverse primer (IDT) and 1 μl DNA. The cycling conditions were as follows: 95°C for 10 min, 16 cycles of 95°C for 30 s, 60°C for 45 s (decrease temperature 0.5°C/cycle), 72°C for 30 s, 34 cycles of 94°C for 20 s, 50°C for 45 s, 72°C for 30 s, and a final elongation at 72°C for 10 min. MSI analysis was performed with a Beckman Coulter sequencer CEQ 8800 (Beckman Coulter, Fullerton, CA, USA) according to the manufacturer's instructions, with 2 μl of PCR product added to each well. Two observers (J.C. and C.D.H.) performed the evaluation of MSI independently, and the results were reported without knowledge of patient history or *hMLH1* or *MGMT* methylation-specific PCR (MSP) status. Any questionable or inconclusive assays were repeated at least once before making a determination.

Loss of heterozygosity (LOH) was determined for samples where the genomic DNA from the normal crypts was heterozygous at a given marker. The ratios of the heterozygous peak-heights were determined for both the normal and ACF samples. LOH was defined as an increase of >50% in the ratio of peak heights for the ACF sample compared to the normal control.

hMLH1 and MGMT MSP

The methylation status of *hMLH1* and *MGMT* was determined by sodium bisulfite treatment of DNA (23) followed by MSP (24). Briefly, 1 μg of salmon sperm DNA was added as a carrier to 10–30 ng of microdissected genomic DNA, or 100 ng of genomic DNA from cell lines, and the total sample volume was brought to 50 μl with nuclease-free H_2O. DNA was denatured with 7.5 μl of 2M NaOH at 37°C for 10 min. DNA was incubated with 3 μl of 100 mM hydroquinone and 540 μl of 3 M sodium bisulfite (pH 5.0) at 50–55°C for 16 h in darkness. After treatment, DNA was purified using the Wizard DNA Cleanup Kit (Promega, Madison, WI, USA) and de-sulfonated with 4.4 μl of 3 M NaOH at 37°C for 15 min. DNA was precipitated with 1/10 volume of 3M sodium acetate (pH 5.2) and 3 volumes 100% ethanol, washed with 70% ethanol, and resuspended in 25 μl nuclease-free water.

For analysis of *hMLH1* promoter methylation, nested PCR was performed to increase reaction sensitivity (Figure 3A). A 376 bp product was amplified in 25 μl volumes using 6 μl bisulfite-treated genomic DNA, ×1 PCR buffer, 37.5 nmol $MgCl_2$, 5 nmol each deoxynucleotide, 0.5 U Platinum *Taq*, and 2.5 pmol forward and reverse primers. The primers used for the first round of PCR, to amplify all bisulfite-treated DNA, were 5'-AGT AGT TTT TTT TTT AGG AGT-3' (sense) and 5'-ATA AAA CCC TAT ACC TAA TCT-3' (antisense). PCR were performed using the following cycling conditions: 95°C for 5 min, 25 cycles of 95°C for 45 s, 47°C for 45 s, and 72°C for 1 min, and extension at 72°C for 10 min. The resulting 376 bp fragment was used as a template for the MSP reaction, using primers as described in Herman *et al*. (25). The 1:100 dilutions of the first PCR were made, and the methylated and unmethylated products were amplified using the same reaction mixture as above. A 115 bp methylated product was amplified using the primers: 5'-ACG TAG ACG TTT TAT TAG GGT CGC-3' (sense) and 5'-CCT CAT CGT AAC TAC CCG CG-3' (antisense). A 124 bp unmethylated product was amplified using the primers: 5'-TTT TGA TGT AGA TGT TTT ATT AGG GTT GT-3' (sense) and 5'-ACC ACC TCA TCA TAA CTA CCC ACA-3' (antisense). The cycling conditions were as follows: 95°C for 5 min, 30 cycles of 95°C for 45 s, 64°C (58°C for the methylated reaction) for 45 s, and 72°C for 1 min, and 72°C for 10 min. All PCR were performed with a control for methylation (RKO cells), a control for no methylation (SW480 cells) and a H_2O control. An aliquot of 25 μl of each PCR was loaded onto a 2% agarose gel, stained with ethidium bromide and visualized under UV illumination.

For analysis of *MGMT* promoter methylation, nested PCR on bisulfite-treated genomic DNA was performed in the same way with the following modifications (Figure 3C). The first round of PCR was performed using a 43°C annealing temperature and amplified a 342 bp product using the following primers: 5'-TRG GAT ATG TTG GGA TAG-3' (sense) and 5'-ACR CCT ACA AAA CCA CT-3' (antisense). *MGMT* MSP was performed using primers described in Esteller *et al*. (26). An 81 bp methylated product was amplified using the following primers: 5'-TTT CGA CGT TCG TAG GTT TTC GC-3' (sense) and 5'-GCA CTC TTC CGA AAA CGA AAC G-3' (antisense) and an annealing temperature of 61°C. A 93 bp unmethylated

product was amplified using the primers: 5'-TTT GTG TTT TGA TGT TTG TAG GTT TTT GT-3' (sense) and 5'-AAC TCC AAC ACT CTT CCA AAA ACA AAA CA-3' (antisense) and an annealing temperature of 58°C. RKO cells were used as a control for the methylated promoter and SW48 cells were used as a control for the unmethylated promoter.

Results

Patients and ACF histology

A total of 45 ACF were biopsied from 20 patients (Table I) undergoing either routine screening colonoscopy or surveillance colonoscopy due to a clinical finding on a previous colonoscopy. This group included 12 patients described as at an elevated risk for colon cancer because of either a family history of colon cancer in at least one first degree relative or a personal history of colon cancer or advanced adenoma (17,18). Patients suspected of having either FAP or HNPCC (based on Amsterdam criteria) were not included in this study. The remaining eight patients indicated no known risk factors for colon cancer. The patients ranged in age from 43 to 86 years (average age = 60). ACF were identified and biopsied from the last 20 cm of the distal colon using a high-resolution close-focus colonoscope and methylene blue staining.

The histopathology of ACF is generally classified into two major categories: hyperplastic and dysplastic (27). Hyperplastic ACF typically display characteristics similar to hyperplastic polyps, often displaying a distinct serrated crypt pattern (Figure 1) (7,20). All but two of the ACF analyzed in our study were hyperplastic, with one lesion being entirely dysplastic and one being composed of both dysplastic and hyperplastic-appearing crypts. While dysplastic ACF are generally better accepted as precursors to CRC, the significance of hyperplastic ACF in tumor progression is less well established (7,20).

MSI identified in ACF

Histologically aberrant crypts were isolated using LCM. Abutting normal-appearing crypts were also laser-captured whenever possible. At least one sample of normal colonic crypts was available from each patient for control purposes. Genomic DNA was extracted from aberrant crypts and normal epithelium, and analyzed using a panel of five microsatellite markers as recommended by the NCI (21), as well as three additional microsatellite markers located within the coding regions of the *hMSH3*, *hMSH6* and *TGFβRII* genes (22) (Figure 2). MSI was identified in at least one marker from 9 of 30 lesions (30%) in the 12 patients at elevated risk for colon cancer (Table I). All nine MSI+ ACF were unstable at <30% of markers tested, consistent with an MSI-low phenotype. One of the elevated risk patients (#9) had a previously identified CRC, but was reported as cancer-free at the time of this study. This patient had two ACF biopsied; one was MSI-low and the other was microsatellite stable (MSS). The presence of MSI in some ACF, but not all, from the same patient was commonly observed (see Table I) and has been reported previously (13). MSI was also detected in 2 of 15 lesions (13%) from the eight average risk patients, both characterized as MSI-high (Table I).

Hypermethylation of DNA repair genes

We examined methylation status of the *hMLH1* promoter from each ACF (Figure 3A and B). *hMLH1* is a mismatch repair (MMR) gene whose expression is deactivated by

Table I. Clinicopathological features of patients, MSI status, hMLH1 and MGMT promoter methylation status and LOH status in ACF

Patient	Age	History[a]	Sample	ACF histology	MSI[b]	Methylation[c]		LOH[d]
						hMLH1	*MGMT*	
Elevated risk patients								
1	86	Ad	042004-1130-3	Hyperplasia	MSS	U	U	—
2	74	Ad	112003-1045-4	Hyperplasia	MSI-L	M	ND	—
			112003-1045-7	Hyperplasia	MSS	U	U	
3	50	Ad	021904-1000-2	Hyperplasia	MSS	M	U	—
			021904-1000-4	Hyperplasia	MSS	U	ND	D5
			021904-1000-5	Hyperplasia	MSS	U	U	—
4	49	FHx	121103-1100-1	Dysplasia	MSI-L	U	M	—
			121103-1100-2	Hyperplasia	MSI-L	M	M	—
			121103-1100-3	Hyperplasia	MSS	U	U	—
5	80	Ad	042604-1130-1	Hyp/dysp	MSS	U	U	—
			042604-1130-3	Hyperplasia	MSS	M	ND	—
			042604-1130-4	Hyperplasia	MSS	M	ND	—
			042604-1130-5	Hyperplasia	MSS	U	U	—
6	56	Ad	071905-930-4	Hyperplasia	MSS	U	U	—
			071905-930-6	Hyperplasia	MSS	M	U	—
7	43	FHx	101804-1100-2	Hyperplasia	MSI-L	U	U	—
			101804-1100-4	Hyperplasia	MSI-L	U	U	—
			101804-100-6	Hyperplasia	MSI-L	U	U	D5
			101804-100-7	Hyperplasia	MSS	ND	ND	—
			101804-1100-12	Hyperplasia	MSI-L	U	U	—
8	79	Ad	101104-1130-1	Hyperplasia	MSI-L	U	U	—
			101104-1130-3	Hyperplasia	MSS	U	U	—
9	76	CRC/FHx	052704-1130-4	Hyperplasia	MSI-L	U	M	—
			052704-1130-5	Hyperplasia	MSS	M	U	—
10	73	Ad	052704-900-2	Hyperplasia	MSS	U	U	—
			052704-900-4	Hyperplasia	MSS	U	ND	—
11	56	Ad	080105-945-2	Hyperplasia	MSS	U	U	—
			080105-945-3	Hyperplasia	MSS	M	U	—
			080105-945-6	Hyperplasia	MSS	U	U	—
12	46	FHx	071204-1130-3	Hyperplasia	MSS	U	U	—
Average risk patients								
1	52	None	2-2	Hyperplasia	MSS	U	ND	—
			2-4	Hyperplasia	MSS	ND	ND	—
2	51	None	3-2	Hyperplasia	MSS	ND	ND	—
			3-3	Hyperplasia	MSS	U	ND	—
			3-5	Hyperplasia	MSS	ND	ND	—
3	58	None	8-3	Hyperplasia	MSS	ND	ND	—
			8-5	Hyperplasia	MSI-H	U	U	—
4	52	None	14-2	Hyperplasia	MSS	U	U	—
			14-3	Hyperplasia	MSI-H	U	U	—
			14-5	Hyperplasia	MSS	U	ND	—
			14-6	Hyperplasia	MSS	U	U	—
5	57	None	16-2	Hyperplasia	MSS	ND	ND	—
6	51	None	24-2	Hyperplasia	MSS	U	ND	—
7	59	None	40-4	Hyperplasia	MSS	U	U	—
8	51	None	042904-1200-2	Hyperplasia	MSS	ND	U	—

[a]Reason for elevated risk status. Ad = advanced adenoma, CRC = colorectal cancer, FHx = family history.
[b]MSI status. MSS = microsatellite stable (instability at 0 markers tested); MSI-L = microsatellite instability-low (instability at 1 or 2 markers tested); MSI-H = microsatellite instability-high (instability at 3 or more markers tested).
[c]Methylation status. M = promoter methylated by MSP; U = promoter unmethylated by MSP; ND = not determined.

promoter hypermethylation in up to 90% of sporadic MSI+ cancers (25,28–30). This epigenetic alteration is thought to be an early event in sporadic colon tumors that arise through a serrated, non-dysplastic adenoma (31,32). We identified *hMLH1* promoter hypermethylation in 8 of 39 (21%) ACF examined (Table I). Whenever possible, we also tested genomic DNA from abutting normal mucosa. We did not find any promoter hypermethylation in normal crypts. Interestingly, we did not see a direct relationship between the presence of *hMLH1* promoter hypermethylation and MSI, as only two of our MSI+ ACF displayed hypermethylation.

Jass and co-workers have posited an association between the MSI-low phenotype and promoter hypermethylation of *MGMT* (33). MGMT is a DNA repair enzyme that removes deleterious methyl adducts from guanine residues. An accumulation of these aberrantly methylated guanines has been shown to activate a MMR-dependent DNA damage response (34), giving rise to the speculation that loss of MGMT in tumors may cause the MMR system to be temporarily overwhelmed resulting in an MSI-low phenotype (33). We tested a subset of our ACF for *MGMT* promoter hypermethylation and report that 3 of 32 (9%) demonstrated hypermethylation (Figure 3C and D, Table I). All three of these ACF displayed an MSI-low phenotype. Similar to *hMLH1*, we did not see any *MGMT* promoter hypermethylation in adjacent normal crypts.
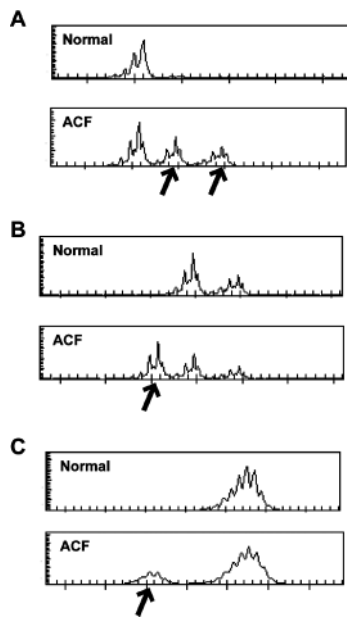
Fig. 2. Examples of MSI detected in ACF in both elevated and average risk patients. (**A**) Genomic DNA from elevated risk patient #5, sample 042604-1130-4 tested for MSI at the D5S346 microsatellite marker. (**B**) Genomic DNA from elevated risk patient #7, sample 101804-1100-2 tested for MSI at the D5S346 microsatellite marker. (**C**) Genomic DNA from average risk patient #4, sample 14-3 tested for MSI at the BAT26 microsatellite marker. MSI indicated by arrows.

LOH identified in ACF

Microsatellite analysis can also be used to assay for LOH. We identified LOH events in two ACF, both from the elevated risk group (Figure 4, Table 1). These LOH events occurred at the D5S346 marker which is near the *APC* tumor suppressor gene.

Discussion

The step-wise progression of CRC from normal mucosa to invasive carcinoma is a process that occurs over many years (16). The ability to recognize the earliest stages of this process may allow for therapeutic intervention to be undertaken that prevents progression to debilitating disease. Although it is widely accepted that adenomas are precursors to CRC, it is unclear what early changes within the colorectal mucosa constitute a bonafide precursor to the adenoma. ACF are generally considered the earliest, identifiable morphological change in the colon, and there is evidence to support the notion that ACF represent CRC precursor lesions (3). As an example, ACF exhibit many of the molecular and genetic abnormalities that form the basis for the adenoma–carcinoma sequence in CRC (7,35). Many of these alterations were discovered in ACF removed during surgery for a concurrent CRC. With the advent of high-resolution, close-focus colonoscopy, it is now possible to identify and biopsy ACF *in situ* allowing for analysis of ACF from patients who have not developed, though may be at risk for developing, CRC.

We report here the identification of MSI in ACF from patients without a concurrent colon cancer. There is an increase in the percentage of MSI+ ACF in patients with a known risk factor for CRC—either a personal history of CRC or advanced adenoma or a family history of CRC in a first-degree relative. First-degree relatives of patients with sporadic CRC have been reported to exhibit an increased risk of developing colon tumors, and this risk increases as the number of affected relatives increases (36). Although the increase we observed in the percentage of MSI+ ACF is not statistically significant ($P \leq 0.25$), it will be interesting to determine whether this trend continues by examining more patients and lesions.

Almost all of the ACF examined in our study, including all but one of the MSI+ ACF, were hyperplastic ACF. The hyperplastic ACF could be the precursor to the hyperplastic polyp that develops during the course of a 'serrated pathway' of sporadic CRC (32). The serrated pathway results in adenocarcinomas typically marked by the presence of MSI, as well as high levels of CpG island methylation in promoter regions of tumor suppressor genes (37). The serrated pathway may include two separate mechanisms that give rise to either MSI-high or MSI-low cancers. Loss of hMLH1 expression due to promoter hypermethylation is commonly observed in MSI-high cancers and some serrated adenomas (38). We have observed *hMLH1* promoter hypermethylation in 8 of 39 ACF. Promoter hypermethylation was never seen in DNA from abutting normal crypts, arguing that this phenomenon is not part of a field effect, but is specific to the lesion. Only two of eight ACF with *hMLH1* promoter hypermethylation displayed MSI. Of the 31 lesions that did not have hypermethylation, 6 displayed MSI, suggesting a lack of significant association in ACF ($P \leq 0.9$). This finding is consistent with a previous report that identified promoter hypermethylation of *hMLH1* in two ACF that were both MSS (15).

The majority of MSI+ ACF identified in the present study were found to be MSI-low. These ACF may represent the earliest stage in an MSI-low cancer pathway. The existence of a separate pathway of tumorigenesis characterized by an MSI-low phenotype has been controversial. The idea stems from observations that tumors with an MSI-low phenotype display different molecular characteristics than MSI-high cancers (33,39,40). One molecular feature of MSI-low cancers is hypermethylation of the *MGMT* promoter (33). We identified *MGMT* promoter hypermethylation in 3/7 MSI-low ACF tested while detecting no hypermethylation in the MSS or MSI-H lesions tested, suggesting an association between *MGMT* promoter hypermethylation and an MSI-L phenotype ($P \leq 0.01$). Loss of MGMT activity may lead to an increase in the number of highly mutagenic O^6-methylguanine lesions in the DNA which, when mispaired with a thymine, activate the MMR pathway (34). Jass *et al*. (32) have proposed that increases in O^6-MeG/T lesions may temporarily overwhelm the MMR system resulting in a transitory mutator phenotype resulting in MSI-L lesions. In general, the nature of the MSI-L phenotype is not clear. While the temporary overwhelming of the MMR pathway is an intriguing model, MSI-L lesions also could potentially arise due to mutations in repair genes that result in a weaker mutator phenotype. As an example, mutations in *hMSH6*, another MMR gene mutated in a small fraction of HNPCC cases, have been proposed to result in a greater frequency of tumors with MSI-L phenotype (41).

Surprisingly, the frequency of MSI+ ACF identified in the present study was somewhat higher than that reported in previous studies of ACF isolated from patients with synchronous cancer (12–14). One possible explanation may be that we are using LCM to isolate aberrant crypts from surrounding stroma and normal mucosa. This technique may
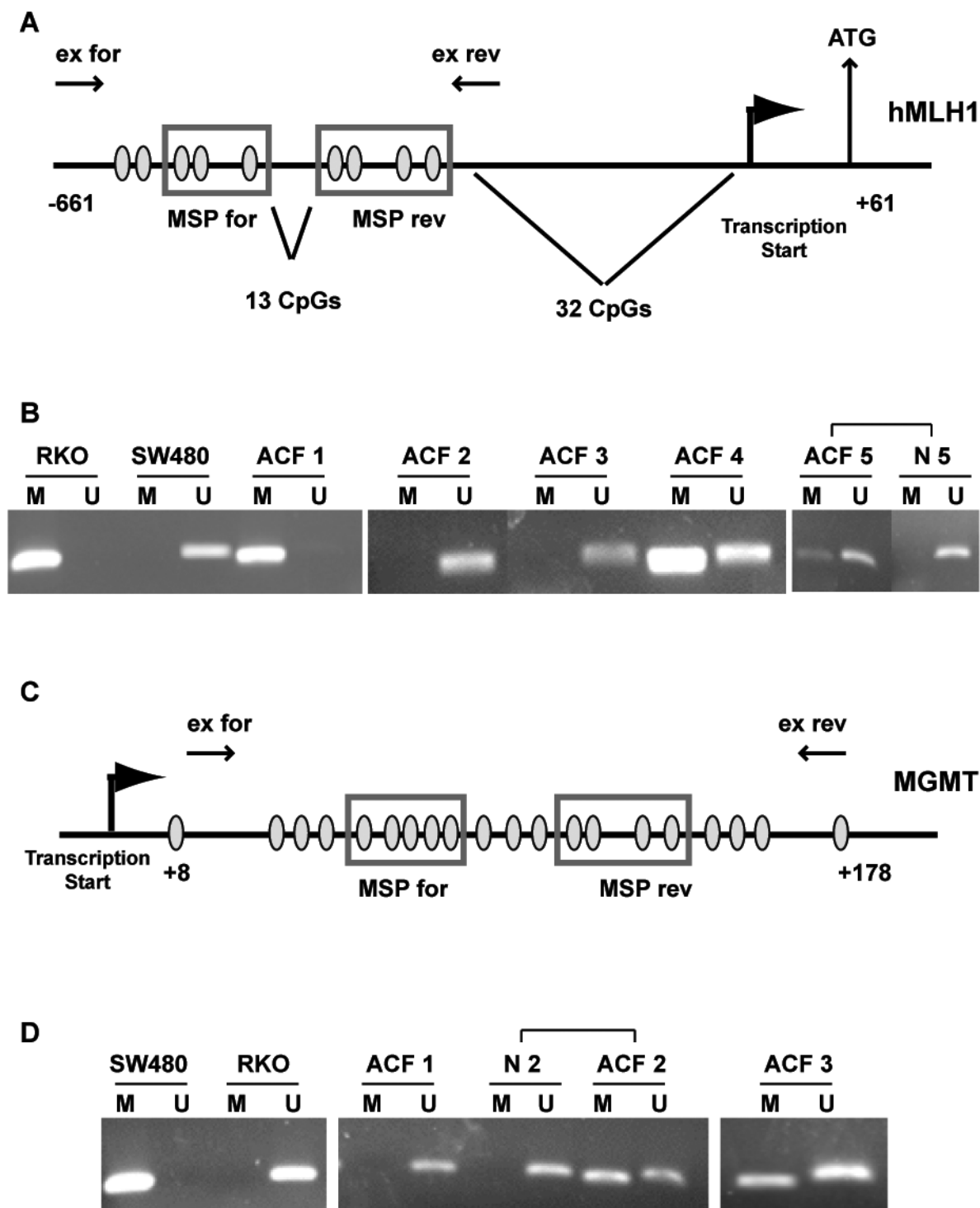
Fig. 3. *hMLH1* and *MGMT* promoter hypermethylation as determined by methylation-specific PCR. (**A** and **C**) Maps of the *hMLH1* and *MGMT* gene promoter regions, respectively, and detail of the CpG islands used for analysis of promoter methylation by MSP (ovals). Arrows marked 'ex for' and 'ex rev' represent the locations of the flanking PCR primers used to amplify a 376 bp template for the *hMLH1* MSP and 342 bp template for *MGMT* MSP. Boxes marked 'MSP for' and 'MSP rev' represent the locations of the methylation-specific primers used to amplify either the methylated promoter (*hMLH1* = 115 bp product; *MGMT* = 81 bp product) or unmethylated promoter (*hMLH1* = 124 bp product; *MGMT* = 93 bp product). (**B**) Representative examples of MSP of *hMLH1* promoter in ACF. MSP was performed using methylation-specific (M) and unmethylation-specific (U) primer sets as detailed in Materials and methods. The presence of a visible PCR product in the lanes marked M indicates the presence of methylated alleles. All samples have variable degrees of amplification with the U primers, most likely due to stromal cell contamination. RKO cells have a fully methylated *hMLH1* promoter and SW480 cells have a fully unmethylated promoter. ACF1 = patient 3, sample 021904-100-2; ACF2 = patient 10, sample 052704-900-2; ACF3 = patient 9, sample 052704-1130-4; ACF4 = patient 9, sample 052704-1130-5; ACF5 = patient 4, sample 121103-1100-2; N5 = the abutting normal mucosa to ACF5. (**D**) As per in (**B**), representative examples of MSP of *MGMT* promoter in ACF. SW48 cells have a fully methylated *MGMT* promoter and RKO cells have a fully unmethylated promoter. ACF1 = patient 3, sample 021904-1000-5; N2 = the abutting normal mucosa to ACF2; ACF2 = patient 4, sample 121103-1100-2; ACF3 = patient 4, sample 121103-1100-1.
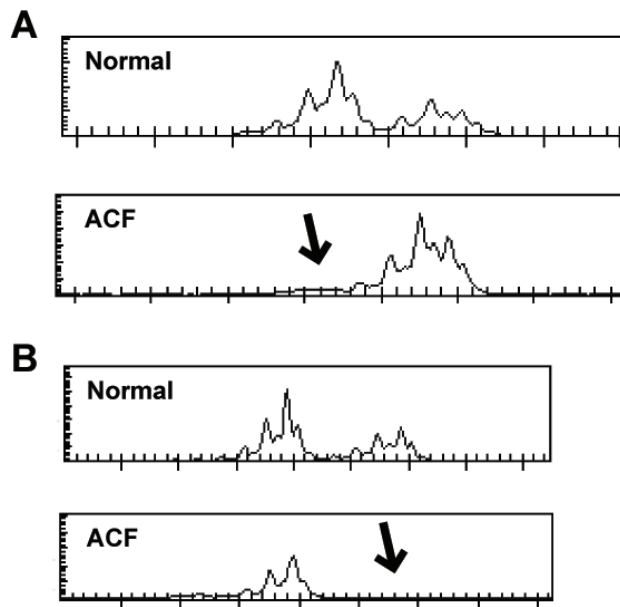
Fig. 4. LOH in ACF at a marker near the *APC* tumor suppressor. LOH was identified in two separate ACF, both at the D5S346 marker on chromosome 5 near the APC tumor suppressor gene. (**A**) LOH identified from elevated risk patient #3, sample 021904-1000-4. (**B**) LOH identified from elevated risk patient #7, sample 101804-100-6. Lost allele indicated by arrows.

increase the sensitivity of our assays, allowing us to detect MSI events that may otherwise have been masked by contaminating DNA from normal cells (42). In addition, all of our biopsied ACF were from the distal 20 cm of the colon. Previous studies focused predominantly on right-sided ACF, where most MSI-high CRC have been located. Some right-sided ACF may not have developed MSI as the MSI-high phenotype appears to arise later in the tumorigenic process (15,39). However, MSI-low cancers and serrated adenomas are typically found on the left side (43). That we find MSI-low ACF more abundantly than MSI-high lesions in the left colon is consistent with these observations and supports the hypothesis that these lesions represent precursors to MSI-low CRC. It is evident, however, that the majority of ACF, even those lesions displaying MSI, do not progress to a carcinoma, or even to an adenoma. In fact, half of all patients have at least one ACF by the time they are 50 years old, and the prevalence and total number of ACF in each patient increases with age (7). Thus, the alternative hypothesis must be considered; that MSI+ ACF, displaying either high or low instability, are less likely to progress to cancer.

Ultimately, the most important clinical question will be to determine whether the presence of MSI+ ACF identified in human subjects offers useful prognostic information regarding cancer risk. While it is neither practical nor even necessary to identify and remove all ACF in every patient who undergo a routine colonoscopy procedure, further studies examining ACF in subsets of patients might lead to information about the effectiveness of chemoprevention agents or other prevention strategies that can halt the tumorigenic process at an early stage.

Acknowledgments

References

1. Bird,R.P. (1987) Observation and quantification of aberrant crypts in the murine colon treated with a colon carcinogen: preliminary findings. *Cancer Lett.*, **37**, 147–151.
2. Pretlow,T.P., Barrow,B.J., Ashton,W.S., O'Riordan,M.A., Pretlow,T.G., Jurcisek,J.A. and Stellato,T.A. (1991) Aberrant crypts: putative preneoplastic foci in human colonic mucosa. *Cancer Res.*, **51**, 1564–1567.
3. Roncucci,L., Pedroni,M., Vaccina,F., Benatti,P., Marzona,L. and De Pol,A. (2000) Aberrant crypt foci in colorectal carcinogenesis. Cell and crypt dynamics. *Cell Prolif.*, **33**, 1–18.
4. Alrawi,S.J., Schiff,M., Carroll,R.E., Dayton,M., Gibbs,J.F., Kulavlat,M., Tan,D., Berman,K., Stoler,D.L. and Anderson,G.R. (2006) Aberrant crypt foci. *Anticancer Res.*, **26**, 107–119.
5. Cheng,L. and Lai,M.D. (2003) Aberrant crypt foci as microscopic precursors of colorectal cancer. *World J. Gastroenterol.*, **9**, 2642–2649.
6. Pretlow,T.P. and Pretlow,T.G. (2005) Mutant KRAS in aberrant crypt foci (ACF): Initiation of colorectal cancer? *Biochim. Biophys. Acta*, **1756**, 83–96.
7. Takayama,T., Katsuki,S., Takahashi,Y., Ohi,M., Nojiri,S., Sakamaki,S., Kato,J., Kogawa,K., Miyake,H. and Niitsu,Y. (1998) Aberrant crypt foci of the colon as precursors of adenoma and cancer. *N. Engl. J. Med.*, **339**, 1277–1284.
8. Hurlstone,D.P. and Cross,S.S. (2005) Role of aberrant crypt foci detected using high-magnification-chromoscopic colonoscopy in human colorectal carcinogenesis. *J. Gastroenterol. Hepatol.*, **20**, 173–181.
9. Liu,B., Parsons,R., Papadopoulos,N. *et al.* (1996) Analysis of mismatch repair genes in hereditary non-polyposis colorectal cancer patients. *Nat. Med.*, **2**, 169–174.
10. Dietmaier,W., Wallinger,S., Bocker,T., Kullmann,F., Fishel,R. and Ruschoff,J. (1997) Diagnostic microsatellite instability: definition and correlation with mismatch repair protein expression. *Cancer Res.*, **57**, 4749–4756.
11. Lubinski,J., Lynch,H.T., Lynch,J. and Shaw,T. (2003) HNPCC (Lynch Syndrome): differential diagnosis, molecular genetics and management—a review. *Hered. Cancer Clin. Prac.*, **1**, 7–18.
12. Augenlicht,L.H., Richards,C., Corner,G. and Pretlow,T.P. (1996) Evidence for genomic instability in human colonic aberrant crypt foci. *Oncogene*, **12**, 1767–1772.
13. Heinen,C.D., Shivapurkar,N., Tang,Z., Groden,J. and Alabaster,O. (1996) Microsatellite instability in aberrant crypt foci from human colons. *Cancer Res.*, **56**, 5339–5341.
14. Pedroni,M., Sala,E., Scarselli,A. *et al.* (2001) Microsatellite instability and mismatch-repair protein expression in hereditary and sporadic colorectal carcinogenesis. *Cancer Res.*, **61**, 896–899.
15. Chan,A.O.-O., Broaddus,R.R., Houlihan,P.S., Issa,J.-P.J., Hamilton,S.R. and Rashid,A. (2002) CpG island methylation in aberrant crypt foci of the colorectum. *Am. J. Pathol.*, **160**, 1823–1830.
16. Fearon,E.R. and Vogelstein,B. (1990) A genetic model for colorectal tumorigenesis. *Cell*, **61**, 759–767.
17. Otchy,D.P., Ransohoff,D.F., Wolff,B.G., Weaver,A., Ilstrup,D., Carlson,H. and Rademacher,D. (1996) Metachronous colon cancer in persons who have had a large adenomatous polyp. *Am. J. Gastroenterol.*, **91**, 448–454.
18. High,E.D., Kim,C. and Cash,B.D. (2005) Yield of index colonoscopy screening in patients <50 years of age with a family history of colorectal cancer: a validation of current screening recommendations. *Gastroenterology*, **128**, S638.
19. Nambiar,P.R., Nakanishi,M., Gupta,R. *et al.* (2004) Genetic signatures of high- and low-risk aberrant crypt foci in a mouse model of sporadic colon cancer. *Cancer Res.*, **64**, 6394–6401.
20. Nucci,M.R., Robinson,C.R., Longo,P., Campbell,P. and Hamilton,S.R. (1997) Phenotypic and genotypic characteristics of aberrant crypt foci in human colorectal mucosa. *Hum. Pathol.*, **28**, 1396–1407.
21. Boland,C.R., Thibodeau,S.N., Hamilton,S.R. *et al.* (1998) A National Cancer Institute Workshop on Microsatellite Instability for cancer detection and familial predisposition: development of international criteria for the determination of microsatellite instability in colorectal cancer. *Cancer Res.*, **58**, 5248–5257.
22. Yamamoto,H., Sawai,H., Weber,T., Rodriguez-Bigas,M. and Perucho,M. (1998) Somatic frameshift mutations in DNA mismatch repair and

proapoptosis genes in hereditary nonpolyposis colorectal cancer. *Cancer Res.*, **58**, 997–1003.

23. Herman,J.G., Graff,J.R., Myohanen,S., Nelkin,B.D. and Baylin,S.B. (1996) Methylation-specific PCR: a novel PCR assay for methylation status of CpG islands. *Proc. Natl Acad. Sci. USA*, **93**, 9821–9826.
24. van Engeland,M., Roemen,G.M., Brink,M., Pachen,M.M., Weijenberg,M.P., de Bruine,A.P., Arends,J.W., van den Brandt,P.A., de Goeij,A.F. and Herman,J.G. (2002) K-ras mutations and RASSF1A promoter methylation in colorectal cancer. *Oncogene*, **21**, 3792–3795.
25. Herman,J.G., Umar,A., Polyak,K. *et al.* (1998) Incidence and functional consequences of hMLH1 promoter hypermethylation in colorectal carcinoma. *Proc. Natl Acad. Sci. USA*, **95**, 6870–6875.
26. Esteller,M., Hamilton,S.R., Burger,P.C., Baylin,S.B. and Herman,J.G. (1999) Inactivation of the DNA repair gene O^6-methylguanine-DNA methyltransferase by promoter hypermethylation is a common event in primary human neoplasia. *Cancer Res.*, **59**, 793–797.
27. Di Gregorio,C., Losi,L., Fante,R., Modica,S., Ghidoni,M., Pedroni,M., Tamassia,M.G., Gafa,L., Ponz de Leon,M. and Roncucci,L. (1997) Histology of aberrant crypt foci in the human colon. *Histopathology*, **30**, 328–334.
28. Veigl,M.L., Kasturi,L., Olechnowicz,J. *et al.* (1998) Biallelic inactivation of hMLH1 by epigenetic gene silencing, a novel mechanism causing human MSI cancers. *Proc. Natl Acad. Sci. USA*, **95**, 8698–8702.
29. Cunningham,J., Christensen,E., Tester,D., Kim,C., Roche,P., Burgart,L. and Thibodeau,S. (1998) Hypermethylation of the hMLH1 promoter in colon cancer with microsatellite instability. *Cancer Res.*, **58**, 3455–3460.
30. Deng,G., Chen,A., Hong,J., Chae,H.S. and Kim,Y.S. (1999) Methylation of CpG in a small region of the hMLH1 promoter invariably correlates with the absence of gene expression. *Cancer Res.*, **59**, 2029–2023.
31. Giovannucci,E. and Ogino,S. (2005) DNA methylation, field effects, and colorectal cancer. *J. Natl Cancer Inst.*, **97**, 1317–1319.
32. Jass,J., Whitehall,V., Young,J. and Leggett,B. (2002) Emerging concepts in colorectal neoplasia. *Gastroenterology*, **123**, 862–876.
33. Whitehall,V.L.J., Walsh,M.D., Young,J., Leggett,B.A. and Jass,J.R. (2001) Methylation of *O-6-methylguanine DNA methyltransferase* characterizes a subset of colorectal cancer with low-level DNA microsatellite instability. *Cancer Res.*, **61**, 827–830.
34. Stojic,L., Brun,R. and Jiricny,J. (2004) Mismatch repair and DNA damage signalling. *DNA Repair*, **3**, 1091–1101.
35. Jen,J., Powell,S.M., Papadopoulos,N., Smith,K.J., Hamilton,S.R., Vogelstein,B. and Kinzler,K.W. (1994) Molecular determinants of dysplasia in colorectal lesions. *Cancer Res.*, **54**, 5523–5526.
36. Burt,R.W. (1999) Impact of family history on screening and surveillance. *Gastrointest. Endosc.*, **49**, S41–44.
37. Jass,J.R. (2001) Serrated route to colorectal cancer: back street or super highway? *J. Pathol.*, **193**, 283–285.
38. Jass,J.R., Iino,H., Ruszkiewicz,A. *et al.* (2000) Neoplastic progression occurs through mutator pathways in hyperplastic polyposis of the colorectum. *Gut*, **47**, 43–49.
39. Wu,M.S., Lee,C.W., Shun,C.T., Wang,H.P., Lee,W.J., Chang,M.C., Sheu,J.C. and Lin,J.T. (2000) Distinct clinicopathologic and genetic profiles in sporadic gastric cancer with different mutator phenotypes. *Genes Chromosomes Cancer*, **27**, 403–411.
40. Mori,Y., Selaru,F.M., Sato,F. *et al.* (2003) The impact of microsatellite instability on the molecular phenotype of colorectal tumors. *Cancer Res.*, **63**, 4577–4582.
41. Wu,Y., Berends,M.J., Mensink,R.G., Kempinga,C., Sijmons,R.H., van Der Zee,A.G., Hollema,H., Kleibeuker,J.H., Buys,C.H. and Hofstra,R.M. (1999) Association of hereditary nonpolyposis colorectal cancer-related tumors displaying low microsatellite instability with MSH6 germline mutations. *Am. J. Hum. Genet.*, **65**, 1291–1298.
42. Greenspan,E.J., Jablonski,M.A., Rajan,T.V., Levine,J., Belinsky,G.S. and Rosenberg,D.W. (2006) Epigenetic alterations in RASSF1A in human aberrant crypt foci. *Carcinogenesis*, **27**, 1316–1322.
43. Jass,J., Biden,K., Cummings,M. *et al.* (1999) Characterisation of a subtype of colorectal cancer combining features of the suppressor and mild mutator pathways. *J. Clin. Pathol.*, **52**, 455–460.